Macromolecules

Volume 38, Number 21 October 18, 2005

Communications to the Editor

Phase Transformation in Self-Assembly of the Gold/Poly(4-vinylpyridine)-*b*-poly(ϵ-caprolactone) Hybrid System

Rong-Ming Ho,*,†,‡ Tao Lin,† Meng-Ru Jhong,† Tsai-Ming Chung,† Bao-Tsan Ko,‡ and Yi-Chun Chen‡

Department of Chemical Engineering, National Tsing-Hua University, Hsinchu 30013, Taiwan, and Union Chemical Laboratories, Industrial Technology Research Institute, Hsinchu 30013, Taiwan

Received June 2, 2005
Revised Manuscript Received August 22, 2005

The self-assembly of soft matters including organic and biological materials is one of the most convenient ways to create nanostructures. The organization of inorganic materials into periodic nanostructures by using soft matters as templates for self-assembling has been thus widely exploited to produce functional hybrid materials, namely nanocompsites.[1−11] The templation of inorganic materials within self-assembly nanostructures is usually achieved by introducing specific interactions such as dipolar interactions, hydrogen bonding, and complex formation between inorganic and organic components. Among them, the self-assembly of inorganic/block copolymer (BCP) hybrid system has been extensively studied. Recently, theoretical simulation in regard to the composite morphology of inorganic/BCP hybrid system was thoroughly carried out by Balazs and coworkers.[12,13] The phase behavior of the hybrid system as a function of diblock composition and inorganic volume fraction were systematically studied. Phase transformation is expected while small size inorganic particles (i.e., the size of inorganic particle is smaller than the dimension of radius of gyration of polymer chains) preferentially interacting with one constituted block are hybridized with BCP. Recently, some experimental results by Kim and co-workers revealed the phase transformation from lamellar to cylinder nanostructure when blending presynthesized nanoparticles with block copolymers at which the inorganic nanoparticles were homogeneously distributed within the preferential microdomains.[14,15] The main objective of this research is to examine the self-assembly behavior, particularly the phase transformation, in inorganic/BCP hybrid system. In this communication, interesting morphological evolution in hybrid system was observed and presented similar behavior to the theoretical predictions in inorganic/block copolymer hybrids[12] and selective solvent/block copolymer blends.[16,17]

A series of diblock copolymers, poly(4-vinylpyridine)-*b*-poly(ϵ-caprolactone), P4VP-*b*-PCL, abbreviated VP/CL *m*/*n* in which *m* and *n* represent the degree of polymerization of each constituted block, respectively, were synthesized via living ring opening and atom-transfer radical polymerization in sequence.[18,19] The $M_{n,P4VP}$ and $M_{n,PCL}$ were characterized with proton nuclear magnetic resonance (^{1}H NMR); the polydispersities index in the final BCPs were determined by gel permeation chromatography (GPC) using standard calibration. The results of characterization are as follows: VP/CL 27/46 (M_n = 2900 g/mol, M_w/M_n = 1.25, $f_{PVP}{}^v$:$f_{PCL}{}^v$ = 37:63). Taking advantages of coordination between the nitrogen lone-pair electrons and gold precursors, the hybridization of inorganic gold precursors and P4VP−PCL can be simply achieved by solution blending. Phase transformation behavior in the self-assembly of the Au/P4VP−PCL hybrid system was experimentally identified.

Bulk samples of block copolymers were prepared by the solution-casting method using dichloromethane (CH_2Cl_2) solution (10 wt % of P4VP−PCL) at room temperature. To eliminate possible effects of PCL crystallization and residual solvent on microphase-separated morphology during solvent evaporation, we annealed all bulk samples at 140 °C, which is above the

† National Tsing-Hua University.
‡ Industrial Technology Research Institute.
* To whom correspondence should be addressed: Tel 886-3-5738349; Fax 886-3-5715408; e-mail rmho@mx.nthu.edu.tw.

10.1021/ma0511447 CCC: $30.25
Published on Web 09/24/2005

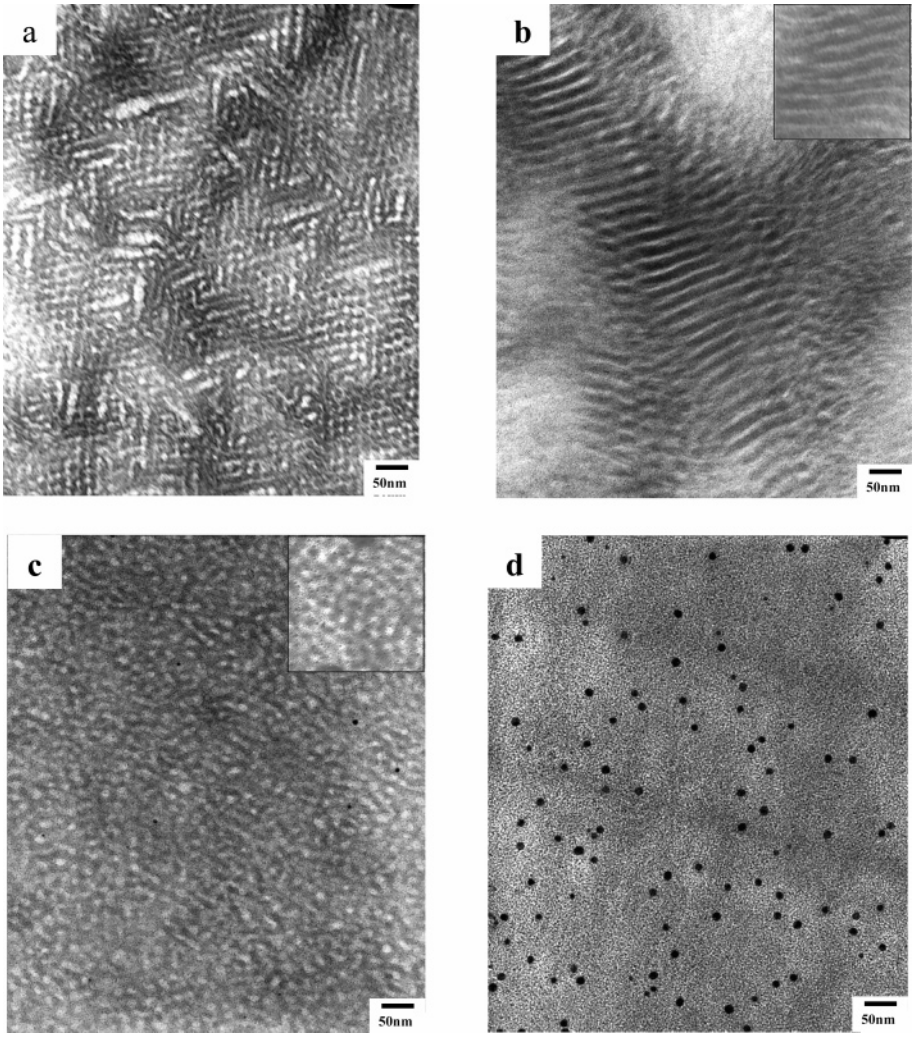

Figure 1. Transmission electron micrographs of RuO_4-stained samples: (a) VP27CL46, (b) VP27CL46 + $HAuCl_4$ (Au/N = 1/7), (c) VP27CL46 + $HAuCl_4$ (Au/N = 1/3), and (d) VP27CL46 + $HAuCl_4$ (Au/N = 1/1). The insets show the TEM micrographs of unstained samples at equal magnification.

glass transition temperature of P4VP blocks ($T_{g,P4VP}$ = 100 °C) and well above the equilibrium melting point ($T_m°_{PCL}$ = 69 °C) of PCL blocks[20] but below estimated order−disorder transition temperature (T_{ODT} ≒ 230 °C),[21] for 12 h under a nitrogen atmosphere. After thermal treatment, the microphase-separated morphology was rapidly cooled at a rate of 150 °C/min to room temperature. The bulk samples of gold/P4VP−PCL hybrids were also prepared by solution casting using dichloromethane (CH_2Cl_2) solution (1 wt % gold/P4VP−PCL) with specific ratio of nitrogen on P4VP block to gold precursor of hydrogen tetrachloroaurate trihydrate ($HAuCl_4$). The solution was stirred for 1 day to allow complete solubilization of the gold precursors. The cast samples were then thermally treated, following the similar procedure for neat BCP samples previously described.

Bright field transmission electron microscopy (TEM) images were obtained using the mass−thickness contrast with a JEOL TEM-1200x transmission electron microscope (at an accelerating voltage of 120 kV). Staining was accomplished by exposing the samples to the vapor of a 4% aqueous RuO_4 solution for 30 min. Small-angle X-ray scattering (SAXS) experiments were conducted at the synchrotron X-ray beamline X27C at the National Synchrotron Light Source (NSLS) in Brookhaven National Laboratory (BNL). The wavelength of the X-ray beam was 0.1366 nm. A MAR CCD X-ray detector (MAR) was used to collect the two-dimensional (2D) SAXS patterns. One-dimensional (1D) linear profile was obtained by integration of the 2D pattern. The scattering angle of the SAXS pattern was calibrated using silver behenate, with the first-order scattering vector q^* ($q^* = 4\pi\lambda^{-1} \sin\theta$, where 2θ is the scattering angle) being 1.076 nm^{-1}. Infrared spectra were recorded on a Perkin-Elmer System-2000 spectrometer at a resolution of 1 cm^{-1}. The experiments were carried out at room temperature (25 °C).

The microphase-separated microstructure of the VP27CL46 ($f_{P4VP}{}^{v}$ = 0.37) sample was examined by TEM and SAXS experiments. As shown in Figure 1a, the microdomains of the P4VP phase appeared dark due to the staining of RuO_4 while the microdomains of PCL appeared light attributed to the crystallinity effect (crystallinity ∼ 50% as measured by differential scanning calorimetry). This TEM result suggests that the microphase-separated morphology exhibits a hexagonally packed cylinder microstructure. Corresponding SAXS pattern further confirmed the observed microstructure. Evaluation of 1D SAXS data (Figure 2a) yielded a long period of microphase-separated hexagonally packed cylinder morphology according to an

expression $D = 2\pi/q^*$ in which the scattering peaks occurred at characteristic q^* ratios of $1:\sqrt{3}$. The spacing of the (100) planes was determined as 18 nm, and the domain spacing was thus 21 nm. The broadening second peak is attributed to the PCL crystalline effect on scattering at which shaper scattering peak can be obtained by in-situ scattering experiment at temperature above PCL melting.

For hybridization, P4VP blocks were used as constituted components to attract gold precursors and stabilize them simultaneously. The incorporation was identified by Fourier transform infrared (FTIR) experiments. As shown in Figure 3, the appearance of extra bands such as 1637 and 1506 cm^{-1} in hybrid samples as compared to neat P4VP−PCL is attributed to the protonation of the pyridine units at which unsaturated gold precursors are coordinated to the nitrogen lone-pair electrons of P4VP.[22] To examine the phase behavior of hybrid system, different amounts of gold precursors were introduced by solution mixing. The added amounts of gold precursors were defined by the stoichiometry of gold precursor vs nitrogen atom used (marked as Au/N) to determine the degree of protonation. Interesting morphological evolution can be observed according to the amounts of gold precursors introduced. At low concentration of gold precursors, the original cylinder morphology was modified by adding gold precursors and finally transformed to lamellar phase while the gold precursors reached critical amount as illustrated in Figure 1b. The gold precursors were uniformly dispersed in the P4VP microdomains as evidenced in the inset of Figure 1b at which the unstained sample appeared significant contrast due to the introduction of high-mass gold precursors. Furthermore, the scattering contrast of microphase-separated microstructure was also enhanced by the introduction of metallic compounds so that significant scattering peaks occurred at characteristic q^* ratios of 1:2:3 were clearly identified (Figure 2b). The long-period spacing of the hybrids (a lamellar nanostructure) was determined as 23 nm, suggesting a recognizable increase in P4VP microdomains. These results reflect that the introduction of gold precursors is preferentially cooperated with the P4VP microdomains and thus induces the transformation of cylinder to lamellae.

Further increasing the concentration of gold precursors, the microphase-separated morphology gradually became disordered-like morphology as shown in Figure 1c (Au/N = 1/3). Consequently, the scattering intensity of SAXS profile from ordered microdomains (Figure 2c) dramatically decreased. Large portions of microphase-separated texture were distorted by the significant coordination of gold precursors and lone-pair electrons. Detailed studies of molecular dispositions with respect to the morphological distortion by the introduction of gold precursors are still in progress. While the added amounts of gold precursor reached Au/N = 1/1, the miscibility of gold precursors and P4VP microdomains was deteriorated due to the excess amounts of gold precursors at which the accommodation of coordination reached maximum allowance and thus led to the occurrence of solubility limit. As a result, gold precursors were found in both components, and noteworthy segregation of gold precursors having size ca. 5 nm, namely segregation of $HAuCl_3$, was observed as shown in Figure 1d. Consequently, disordered scattering (Figure 2d) was thus obtained.

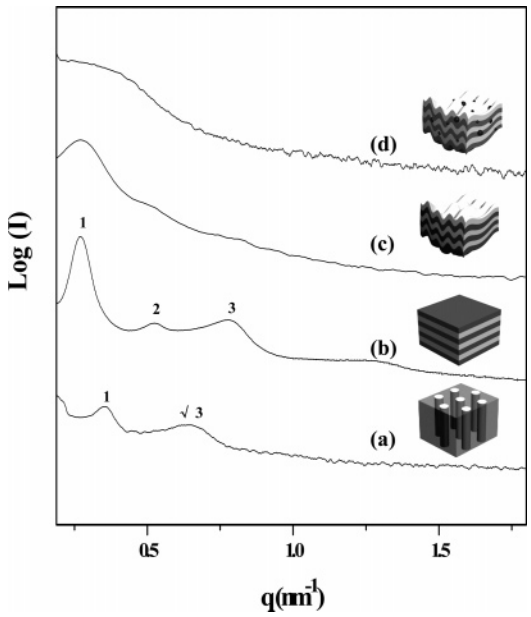

Figure 2. One-dimensional SAXS profiles of (a) VP27CL46, (b)VP27CL46 + $HAuCl_4$ (Au/N = 1/7), (c) VP27CL46 + $HAuCl_4$ (Au/N = 1/3), and (d) VP27CL46 + $HAuCl_4$ (Au/N = 1/1).

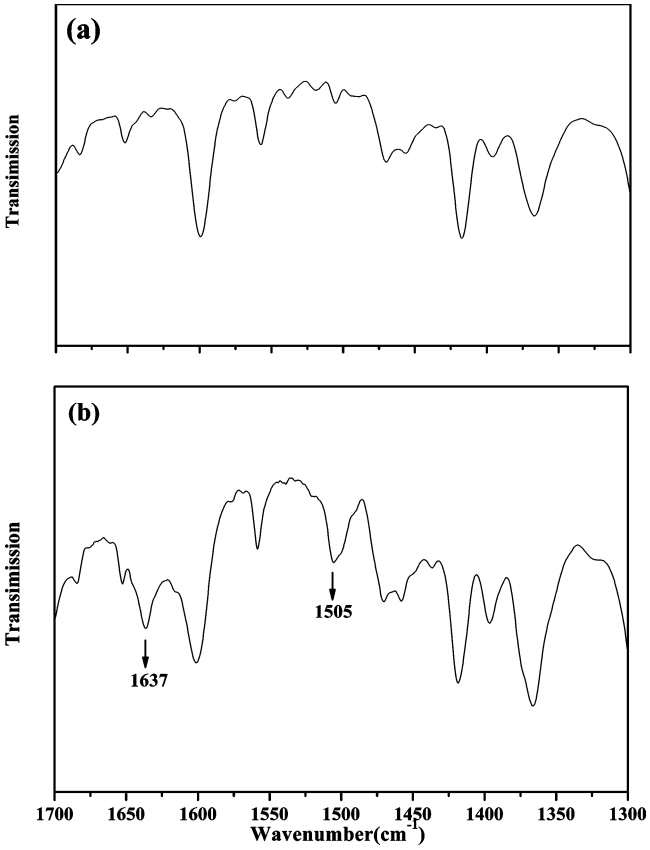

Figure 3. FTIR spectrum of (a) VP27CL46 ($f_{P4VP}{}^{v} = 0.37$) and (b) VP27CL46 + $HAuCl_4$ (Au/N = 1/7).

Interestingly, the phase transformation behavior is consistent with the theoretical prediction in the inorganic/BCP hybrid system. As predicted by Balazs and coworkers, the introduction of inorganic component to the block copolymer materials gives rise to the change on hybridized morphology due to the preferential particle and constituted block interactions and particle−particle excluded-volume interactions as well as enthalpic and entropic interactions within the blocks. For the gold/

P4VP hybrid system studied, the gold precursors size are much smaller than the radius of gyration of constituted block, and the gold precursors are preferentially interacted with P4VP blocks. On the basis of strong segregation condition, gold precursors are expected to be homogeneously distributed within the preferred P4VP microdomains so as to induce phase transformation of microphase-separatred morphology due to the excluded-volume consideration; the observed phase behavior is exactly consistent with the theoretical predictions. This phase behavior also agrees qualitatively with theoretical calculations for the morphological evolution of diblock copolymers with selective solvents which presumably act much like small particles. As increasing the volume fraction of gold precursors, the segregation of gold precursors from the diblock copolymers occurred, and the system exhibited mixed morphology including the segregated particles and the distorted microphase-separated morphology as well as randomly distributed gold precursors.

In conclusion, interesting morphological evolution was observed by introducing various amounts of gold precursors to poly(4-vinylpyridine)-*b*-poly(ϵ-caprolactone) (P4VP−PCL) diblock copolymers. As evidenced by TEM and SAXS, distinct phase transformation from cylinder to lamellae can be identified in the hybrid system of gold/P4VP−PCL due to the preferential wetting of gold precursors in the P4VP microdomains. Further increasing the adding amounts of gold precursors, the microphase-separated morphology of the P4VP−PCL might be destructed by significant coordination between gold precursors and the nitrogen lone-pair electrons of P4VP. Eventually, noteworthy aggregation of gold precursors occurred due to the induced immiscibility between gold precursor and block copolymer. Consistent with the theoretical prediction of inorganic/block copolymer and selective solvent/block copolymer morphology, the observed transformation for the hybrid system of gold/P4VP−PCL is attributed to the excluded volume of gold precursors and its preferential interaction with the P4VP blocks.

Acknowledgment. We thank Dr. B. S. Hsiao of the Chemistry Department, State University of New York at Stony Brook, and Drs. S. Ran and I. Sics of the National Synchrotron Light Source at Brookhaven National Laboratory for their help with Synchrotron SAXS experiments. Our appreciation is extended to Ms. P.-C. Chao of Regional Instruments Center at NCHU for her help with TEM experiments.

References and Notes

(1) Spatz, J. P.; Roescher, A.; Moller, M. *Adv. Mater.* **1996**, *8*, 337.
(2) Forster, S.; Antonietti, M. *Adv. Mater.* **1998**, *10*, 195.
(3) Thurn-Albrecht, T.; Schotter, J.; Kastle, G. A.; Emley, N.; Shibauchi, T.; krusin-Elbaum, L.; Guarini, K.; Black, C. T.; Tuominen, M. T.; Russell, T. P. *Science* **2000**, *290*, 2126.
(4) Lopes, W. A.; Jaeger, M. *Nature (London)* **2001**, *414*, 735.
(5) Bockstaller, M. R.; Kolb, R.; Thomas, E. L. *Adv. Mater.* **2001**, *13*, 1783.
(6) Ribbe, A. E.; Okumura, A.; Matsushige, K.; Hashimoto, T. *Macromolecules* **2001**, *34*, 8239.
(7) Sohn, B. H.; Seo, B. H. *Chem. Mater.* **2001**, *13*, 1752.
(8) Boontongkong, Y.; Cohen, R. E. *Macromolecules* **2002**, *35*, 3647.
(9) Abes, J. I.; Cohen, R. E.; Ross, C. A. *Chem. Mater.* **2003**, *15*, 1125.
(10) Yeh, S. W.; Wei, K. H.; Sun, Y. S.; Jeng, U. S.; Liang, K. S. *Macromolecules* **2003**, *36*, 7903.
(11) Bockstaller, M. R.; Thomas, E. L. *Phys. Rev. Lett.* **2004**, *93*, 166106.
(12) Huh, J.; Ginzburg, V. V.; Balazs, A. C. *Macromolecules* **2000**, *33*, 8085.
(13) Thompson, R. B.; Ginzburg, V. V.; Matsen, M. W.; Balazs, A. C. *Science* **2001**, *292*, 2469.
(14) Kim, B. J.; Chiu, J. J.; Yi, G.-R.; Pine, D. J.; Kramer, unpublished results.
(15) Bockstaller, M. R.; Mickiewicz, R. A.; Thomas, E. L. *Adv. Mater.* **2005**, *17*, 1331.
(16) Hanley, K. J.; Lodge, T. P. *J. Polym. Sci., Polym. Phys. Ed.* **1998**, *36*, 3101.
(17) Hanley, K. J.; Lodge, T. P.; Huang, C. I. *Macromolecules* **2000**, *33*, 5918.
(18) Ko, B. T.; Lin, C. C. *Macromolecules* **1999**, *32*, 8296.
(19) Xia, J.; Zhang, X.; Matyjaszewski, K. *Macromolecules* **1999**, 32, 3531.
(20) Brandrup, J.; Immergut, H. *Polymer Handbook*; Wiley: New York, 1989.
(21) According to the method to determine χ by measuring the characteristic domain spacing (D_{lam}) from SAXS patterns for lamellar morphology, symmetric BCP P4VP-*b*-PCL (VP/CL 47/46, $f^{v}_{PCL} = 0.5$) served to determine the temperature dependence of χ that is described by $\chi(T) = 103.48/T - 0.062$. The order−disorder transition temperatures for P4VP-*b*-PCL samples tested here were determined from SAXS at various temperatures at and above 120 °C to avoid nonequilibrium effects below the glass transition of P4VP. The BCP synthesized is expected not to disorder up to their decomposition point (>200 °C) on the basis of the block chain length and in-situ SAXS evidence.
(22) Antoneitti, M.; Wenz, E.; Bronstein, L.; Seregina, M. *Adv. Mater.* **1995**, *7*, 1000.

MA0511447